

1 **Functional correlates of immediate early gene expression in mouse visual cortex**

2 David Mahringer^{1,2}, Pawel Zmarz^{1,2,3}, Hiroyuki Okuno⁴, Haruhiko Bito⁵ & Georg B. Keller^{1,2,6}

3 ¹ *Friedrich Miescher Institute for Biomedical Research, Basel, Switzerland.*

4 ² *Faculty of Natural Sciences, University of Basel, Basel, Switzerland.*

5 ³ *Current address: Department of Organismic and Evolutionary Biology and Center for Brain Science,*
6 *Harvard University, Cambridge, MA 02138, USA.*

7 ⁴ *Department of Biochemistry and Molecular Biology, Kagoshima University Graduate School of Medical*
8 *and Dental Sciences, Kagoshima, Kagoshima 890-8544, Japan.*

9 ⁵ *Department of Neurochemistry, Graduate School of Medicine, The University of Tokyo, Hongo 7-3-1,*
10 *Bunkyo-ku, Tokyo 113-0033, Japan.*

11 ⁶ Lead contact: georg.keller@fmi.ch

12

13 **During visual development, response properties of layer 2/3 neurons in visual cortex are shaped by**
14 **experience. Both visual and visuomotor experience are necessary to coordinate the integration of**
15 **bottom-up visual input and top-down motor-related input. Whether visual and visuomotor**
16 **experience engage different plasticity mechanisms, possibly associated with the two separate input**
17 **pathways, is still unclear. To begin addressing this, we measured the expression level of three**
18 **different immediate early genes (IEG) (*c-fos*, *egr1* or *Arc*) and neuronal activity in layer 2/3 neurons of**
19 **visual cortex before and after a mouse's first visual exposure in life, and subsequent visuomotor**
20 **learning. We found that expression levels of all three IEGs correlated positively with neuronal activity,**
21 **but that first visual and first visuomotor exposure resulted in differential changes in IEG expression**
22 **patterns. In addition, IEG expression levels differed depending on whether neurons exhibited**
23 **primarily visually driven or motor-related activity. Neurons with strong motor-related activity**
24 **preferentially expressed EGR1, while neurons that developed strong visually driven activity**
25 **preferentially expressed Arc. Our findings are consistent with the interpretation that bottom-up visual**
26 **input and top-down motor-related input are associated with different IEG expression patterns and**
27 **hence possibly also with different plasticity pathways.**

28 **** Dear reader, please note this manuscript is formatted in a standard submission format. ****

29 **INTRODUCTION**

30 During first visuomotor exposure in life, experience with coupling between movement and visual
31 feedback is thought to coordinate inputs onto layer 2/3 neurons in primary visual cortex (V1) such that

32 individual neurons receive balanced and opposing top-down motor-related and bottom-up visual input
33 (Attinger et al., 2017; Jordan and Keller, 2020; Leinweber et al., 2017). While visual input without
34 visuomotor coupling is sufficient to establish normal visual responses in layer 2/3 neurons, the
35 emergence of visuomotor mismatch responses is contingent on experience with visuomotor coupling
36 (Attinger et al., 2017) and relies on NMDA receptor dependent signaling in the local V1 circuit (Widmer
37 et al., 2022). How top-down and bottom-up inputs are coordinated during visual and visuomotor
38 experience and whether plasticity mechanisms in the bottom-up visual driven pathway are the same as
39 those engaged in the top-down motor-related input is still unclear. Here we set out to test for changes
40 in expression levels of immediate early gene (IEG) products in functionally identified neurons during first
41 exposure to visual input and first exposure to normal visuomotor coupling using concurrent
42 measurement of neuronal activity and IEG expression levels in layer 2/3 of mouse visual cortex.

43 IEG products play a critical role in synaptic and neuronal plasticity during learning (Chowdhury et al.,
44 2006; Fleischmann et al., 2003; Gandolfi et al., 2017; Jones et al., 2001; Messaoudi et al., 2007; Rial
45 Verde et al., 2006; Shepherd and Bear, 2011; Shepherd et al., 2006; Tzingounis and Nicoll, 2006;
46 Vazdarjanova et al., 2006; Veyrac et al., 2014; Waung et al., 2008) and are necessary for long-term
47 memory consolidation (Bozon et al., 2003; Fleischmann et al., 2003; Guzowski, 2002; Guzowski and
48 McGaugh, 1997; Guzowski et al., 2000; Jones et al., 2001; Ploski et al., 2008; Yasoshima et al., 2006).
49 Ever since the discovery that the expression of the transcription factor c-Fos can be induced by electrical
50 or chemical stimulation in neurons (Greenberg and Ziff, 1984), the expression of IEGs has been used as a
51 marker for neuronal activity (Bullitt, 1990; Guzowski et al., 1999; Jarvis et al., 2000; Knapska and
52 Kaczmarek, 2004; Minatohara et al., 2015; Morgan et al., 1987; Ramírez-Amaya et al., 2005;
53 Reijmers et al., 2007; Wang et al., 2021). Based on the discovery that certain forms of episodic
54 memory can be reactivated by artificially activating an ensemble of neurons characterized by high IEG
55 expression levels during memory acquisition (Denny et al., 2014; Garner et al., 2012; Liu et al., 2012;
56 Ramirez et al., 2013), it has been speculated that IEG expression is related not simply to neuronal
57 activity *per se*, but to the induction of activity-dependent plasticity (Holtmaat and Caroni, 2016; Josselyn
58 et al., 2015; Kaplan et al., 1996). Assuming IEG expression is indeed related to the induction of neuronal
59 plasticity, it is conceivable that different IEGs are preferentially involved in plasticity of different synapse
60 types or input pathways. c-Fos and EGR1 expression levels in visual cortex, for example, are differentially
61 regulated by visual experience and exhibit a differential dependence on neuromodulatory input
62 (Yamada et al., 1999). Consistent with a pathway-specific role of Arc and EGR1 in visual cortex, it has

63 been shown that Arc is necessary for different forms of plasticity of bottom-up visual input, including
64 ocular dominance plasticity (Gao et al., 2010; Jenks et al., 2017; McCurry et al., 2010; Wang et al., 2006),
65 while a knockout of *egr1* has been shown to leave ocular dominance plasticity unaffected (Mataga et al.,
66 2001), and EGR1 expression levels have been shown to be modulated in a context-specific manner,
67 primarily in a subset of superficial layer 2/3 neurons (Xie et al., 2014). It is still unclear however, whether
68 IEG expression is differentially regulated by changes in bottom-up and top-down input and if there is
69 preferential expression of different IEGs in neurons that are predominantly excited by top-down motor-
70 related input as compared to neurons that are predominantly excited by bottom-up visual input.

71 RESULTS

72 To measure both IEG expression levels and neuronal activity chronically, we used a combination of
73 transgenic mice that express GFP under the control of an IEG promoter and viral delivery of a red variant
74 of a genetically encoded calcium indicator. We did this for three different IEGs (*c-fos*, *egr1*, and *Arc*), in
75 three groups of mice separately. EGFP-Arc and c-Fos-GFP mice are transgenic mice that express a fusion
76 protein of Arc or c-Fos, and GFP downstream of either an *Arc* or a *c-fos* promoter, respectively (Barth et
77 al., 2004; Okuno et al., 2012), while the EGR1-GFP mouse expresses GFP under an *egr1* promoter (Xie et
78 al., 2014). Although there are a number of caveats to using GFP levels in these mouse lines as a proxy for
79 IEG expression levels (see Discussion), there is a strong overlap between post-mortem antibody staining
80 for the respective IEG and GFP expression in all three mouse lines (Barth et al., 2004; Okuno et al., 2012;
81 Xie et al., 2014; Yassin et al., 2010). Throughout the manuscript, we will use IEG expression to mean GFP
82 expression levels in these mice. To measure calcium activity, we used an AAV2/1-Ef1a-jRGECO1a viral
83 vector to express the genetically encoded red calcium indicator jRGECO1a (Dana et al., 2016). This
84 biased our recordings to excitatory neurons, as in the first few weeks after the injection, the Ef1a
85 promoter restricts expression mainly to excitatory neurons (Attinger et al., 2017).

86 To quantify the correlation between neuronal activity and IEG expression of individual neurons in layer
87 2/3 of visual cortex in adult mice, we first used a paradigm of dark adaptation and subsequent brief
88 visual exposure (**Figure 1A**). We did this in three groups of adult mice separately (4 EGFP-Arc mice, 4 c-
89 Fos-GFP mice, and 4 EGR1-GFP mice, between 100 and 291 days old). We dark-adapted all three groups
90 of mice for 24 hours and subsequently head-fixed them, while still in complete darkness, under a two-
91 photon microscope on a spherical treadmill (**Figure 1A**). We then measured calcium activity and IEG
92 levels every 15 minutes for six hours (**Figures 1B-1D**; see Methods). Between the first and second
93 measurement, mice were exposed to visual input for 15 minutes. This paradigm, which is a combination

94 of light exposure and exposure of the mouse to head-fixation, resulted in transient and modest
95 increases in Arc and EGR1 expression levels, and a decrease in c-Fos expression levels (**Figure S1A**).
96 Given that mean neuronal activity levels in V1 are rapidly stabilized across light-dark transitions (Hengen
97 et al., 2016), and only a prolonged dark adaption (of 60 hours) results in a substantial increase of
98 neuronal activity upon light exposure (Torrado Pacheco et al., 2019), the absence of a response in mean
99 IEG levels is perhaps not surprising. We then computed the correlation between average neuronal
100 activity and IEG expression levels for each neuron as a function of time between neuronal activity
101 measurement and IEG expression measurement (**Figures 1E-1G**). Correlation peaked at a time lag of
102 approximately $3.5 \text{ h} \pm 0.5 \text{ h}$ (mean \pm SEM) between neuronal activity measurement and IEG
103 measurement for Arc and c-Fos, and was positive but relatively stable in a window from -2 hours to +3
104 hours for EGR1, consistent with previous results (Wang et al., 2021) (Arc: 1382 neurons, c-Fos: 1070
105 neurons, EGR1: 1319 neurons; **Figures 1E-1G**). At peak, the correlation between neuronal activity and
106 IEG expression was highest for c-Fos, intermediate for Arc, and lowest for EGR1 (**Figures 1H-1J**;
107 correlation coefficients for c-Fos: 0.39 ± 0.07 , Arc: 0.26 ± 0.05 , EGR1: 0.21 ± 0.03 , mean \pm SEM;
108 comparisons between c-Fos vs. Arc: $p < 3 \times 10^{-4}$, Arc vs. EGR1: $p = 0.0188$, c-Fos vs. EGR1: $p < 10^{-8}$; 4 mice
109 per group, t-test with bootstrapping, see Methods). The positive correlation and the time lag of the
110 correlation peak would be consistent with the idea that neuronal activity induces IEG expression, but
111 the fact that correlations with mean activity were relatively weak could mean that it is specific patterns
112 or types of activity that induce IEG expression. It is often assumed that IEG expression is also a correlate
113 of neuronal plasticity (Holtmaat and Caroni, 2016; Josselyn et al., 2015; Kaplan et al., 1996). Given that
114 certain forms of neuronal plasticity are associated with bursts of activity, we first tested whether
115 maximum activity was a better predictor of IEG expression levels than mean activity. Indeed, we found
116 that the correlation with maximum neuronal activity was higher than the correlation with mean activity
117 for all three IEGs, but only significantly so for Arc and EGR1 (**Figure S1B**). Thus, while there is a weak but
118 positive correlation between calcium activity and IEG expression for all three IEGs, it is possible that IEG
119 expression is more directly related to functional plasticity.

120 In visual cortex, both first visual and first visuomotor exposure are associated with significant changes in
121 functional responses (Attinger et al., 2017). To investigate whether visual and visuomotor exposure are
122 also associated with differential expression of IEGs, we proceeded to apply the same methods of
123 measuring IEG dynamics and neuronal calcium activity during a mouse's first exposure to visual input
124 and subsequent first exposure to normal visuomotor coupling. We reared mice in complete darkness
125 and quantified both IEG expression levels and neuronal activity before and after mice were exposed to

126 visual input for the first time in life as well as during a subsequent phase of visuomotor learning. Under
127 normal conditions, first visual exposure is coincident with exposure to normal visuomotor coupling. At
128 eye opening, mice are capable of moving eyes, head, and body and thus immediately experience self-
129 generated visual feedback. To experimentally separate the moment of first visual exposure from first
130 exposure to normal visuomotor coupling, we recorded neuronal activity and IEG expression as mice
131 transitioned through three different experimental conditions. Prior to experiments, three groups of mice
132 were reared in complete darkness until postnatal day 40 (7 EGFP-Arc mice, 5 c-Fos-GFP mice, and 4
133 EGR1-GFP mice). We then imaged neuronal activity and IEG expression levels every 12 hours for a total
134 of 6 days. During all two-photon imaging experiments, mice were head-fixed on a spherical treadmill.
135 During the first four recording sessions, mice were kept on the setup in darkness to measure
136 locomotion-related and non-visual activity and remained dark housed in between recording sessions
137 (condition 1). At the beginning of the 5th recording session, mice were then exposed to visual input for
138 the first time in their life. In the subsequent four recording sessions, mice were exposed to different
139 virtual environments but remained housed in darkness in the time between the recording sessions
140 (condition 2). In addition to recording activity in darkness, recording sessions in condition 2 also
141 contained 8 min of closed-loop feedback during which visual flow on the walls of a virtual corridor was
142 coupled to the mouse's locomotion on the spherical treadmill. During closed-loop feedback, we added
143 brief halts of visual flow to probe for visuomotor mismatch responses (Keller et al., 2012). This was
144 followed by a phase of open-loop feedback during which the visual flow generated by the mouse during
145 the closed-loop feedback was replayed independently of the locomotion of the mouse. Lastly, we
146 presented a series of drifting gratings to the mouse to quantify visual responses (see Methods).
147 Following recording session 8, mice were introduced to a normal 12 h light / 12 h dark cycle. At this
148 time, mice first experienced normal visuomotor coupling in their home cage. We continued recording
149 for an additional four sessions (condition 3) with the same series of closed-loop, open-loop and grating
150 stimulation phases as in condition 2 (**Figure 2A**). Recording sessions lasted on average 12 min \pm 0.5 min
151 (mean \pm SEM) in condition 1, and 83 min \pm 1 min (mean \pm SEM) in conditions 2 and 3 (**Figure S2**). Note,
152 to probe for different visuomotor mismatch responses, condition 2 already contains a short period of
153 head-fixed, closed-loop feedback. Given the short duration and the fact that coupling here is only in a
154 small subspace (forward locomotion coupled to backward visual flow and normal coupling for eye
155 movements) of the total space of visuomotor coupling, we would expect the exposure to normal
156 visuomotor coupling in condition 3 to have a stronger influence on visuomotor integration. The aim of

157 this paradigm was to experimentally separate the first visual exposure at the beginning of condition 2,
158 from the first exposure to normal visuomotor coupling at the beginning of condition 3.

159 It has been shown that visual input can drive the expression of different IEGs in a subset of neurons in
160 visual cortex (Kaminska et al., 1996; Kawashima et al., 2013; Rosen et al., 1992; Tagawa et al., 2005;
161 Wang et al., 2006). Based on this it is sometimes assumed that neuronal activity in visual cortex is higher
162 with visual input than it is in darkness. Differences in neuronal activity between light and dark, however,
163 are small and predominantly transient (Fiser et al., 2004; Hengen et al., 2016; Torrado Pacheco et al.,
164 2019). To test whether in our paradigm first visual exposure or first exposure to normal visuomotor
165 coupling results in an increase of average neuronal activity in visual cortex, we quantified average
166 neuronal activity in each recording session (in condition 1 this only included recordings in darkness,
167 while in conditions 2 and 3 this included recordings in darkness, closed and open-loop feedback, as well
168 as drifting gratings). Consistent with a strong motor-related drive in visual cortex (Keller et al., 2012;
169 Saleem et al., 2013) and rapid homeostatic restoration of average activity following removal of visual
170 input (Keck et al., 2013), we found no evidence of an increase of average neuronal activity at the onset
171 of either condition 2 (first visual exposure) or condition 3 (first exposure to normal visuomotor coupling)
172 (**Figure 2B**). To the contrary, following the first visual exposure, there was a trend for decreasing activity
173 levels ($p = 0.0293$, $R^2 = 0.371$, linear trend analysis, see Methods). We next quantified average
174 expression of Arc, c-Fos and EGR1 over the same time course. Consistent with the absence of a change
175 in average activity levels, we found no significant changes in the expression levels of any of the three
176 IEGs following the first visual exposure at the beginning of condition 2 (**Figure 2C**). Note, we cannot
177 exclude that there is a transient increase in IEG expression between 1 h and 12 h following first visual
178 exposure, as we only recorded for 1 hour every 12 hours. We did however find that the first exposure to
179 normal visuomotor coupling at the beginning of condition 3, resulted in an increase in the expression of
180 Arc and a decrease in the expression of EGR1 in the absence of a measurable change in average
181 neuronal activity levels (**Figure 2C**). To test for changes in the pattern of IEG expression, we quantified
182 the similarity of IEG expression patterns by computing the correlation of IEG expression vectors
183 between imaging time points (see Methods). We found that the pattern of Arc expression changed both
184 with the first visual exposure (onset of condition 2) and the first exposure to normal visuomotor
185 coupling (onset of condition 3) (**Figure 2D**). The pattern of c-Fos expression exhibited no detectable
186 discontinuous changes (**Figure 2E**), while the pattern of EGR1 expression exhibited a marked transition
187 with the first exposure to normal visuomotor coupling (onset of condition 3) (**Figure 2F**). This suggests

188 that the expression patterns of IEGs are differentially and dynamically regulated by visuomotor
189 experience, also in absence of population mean expression level changes.

190 Neurons in layer 2/3 of primary visual cortex are driven differentially by visual and motor-related inputs
191 (Attinger et al., 2017; Keller et al., 2012; Leinweber et al., 2017). Given that the expression patterns of
192 the three IEGs are differentially altered by first visual exposure and first exposure to normal visuomotor
193 coupling, we speculated that the different IEGs could be preferentially expressed in different functional
194 types of excitatory neurons in layer 2/3. Neurons that are more strongly visually driven, likely by
195 bottom-up visual input, could have a different IEG expression profile than neurons that are more
196 strongly driven by top-down motor-related signals (Leinweber et al., 2017; Makino and Komiyama,
197 2015). To test this, we quantified the functional properties of the neurons with the highest IEG
198 expression levels immediately after the first exposure to normal visuomotor coupling where we
199 observed the largest mean IEG expression level changes (**Figure 2C**). We selected the 10 % of neurons
200 with the highest Arc, c-Fos and EGR1 expression, respectively, at the beginning of condition 3 (Arc: 197
201 neurons, c-Fos: 189 neurons, EGR1: 121 neurons) and tested whether these neurons were more strongly
202 driven by visual or motor-related input. As a measure of the strength of the motor-related input, we
203 used the magnitude of the neuronal response during running onsets in darkness. We found that on
204 average neurons with high EGR1 expression levels developed higher motor-related responses than the
205 rest of the population in both condition 2 and condition 3. Conversely, neurons with high Arc expression
206 levels on average developed motor-related responses that are lower than the rest of the population
207 following exposure to normal visuomotor coupling. Responses in neurons with high c-Fos expression
208 levels were not different from responses in the rest of the population (**Figure 3A**). To quantify the
209 strength of visual input we used the magnitude of the neuronal response to drifting grating stimuli.
210 Consistent with the fact that Arc expression can be selectively induced by visual stimuli in a stimulus-
211 specific manner (Kawashima et al., 2013), we found that neurons with high Arc expression levels
212 developed responses to drifting grating stimuli that were on average stronger than the rest of the
213 population after exposure to normal visuomotor coupling. The drifting grating responses of neurons
214 with high EGR1 or c-Fos expression levels were not different from the mean population response (**Figure**
215 **3B**). Thus, neurons with high levels of EGR1 expression after first exposure to normal visuomotor
216 coupling were more strongly driven by motor-related input, while those with high levels of Arc
217 expression were more strongly driven by visual input.

218 One of the signals that has been speculated to be computed in mouse primary visual cortex that
219 combines visual and motor-related input is visuomotor mismatch (Attinger et al., 2017; Keller et al.,
220 2012; Zmarz and Keller, 2016). Neurons that respond to mismatch, or negative prediction errors, are
221 thought to receive excitatory motor-related input and inhibitory visual input (Attinger et al., 2017; Keller
222 and Mrcic-Flogel, 2018). We speculated that given the increased motor-related activity in neurons that
223 express high levels of EGR1, neuronal activity in these neurons should correlate positively with running,
224 while activity in neurons that express high levels of Arc should correlate positively with visual flow. To
225 quantify this, we computed the correlation of neuronal activity with either running or visual flow during
226 the open-loop phases in conditions 2 and 3 for the three groups of neurons with high IEG expression
227 levels. We found that the activity of neurons expressing high levels of EGR1 correlated most strongly
228 with running, while the activity of neurons with high levels of Arc expression correlated positively with
229 visual flow (**Figure 4A**). Consistent with this we found that visuomotor mismatch responses were larger
230 in neurons with high EGR1 expression than in the rest of the population, while they were lower in
231 neurons with high Arc expression than in the rest of the population (**Figure 4B**). This indicates that, at
232 the onset of normal visuomotor coupling, EGR1 is preferentially expressed in mismatch neurons or,
233 more generally, in neurons that are driven by excitatory top-down input, while Arc is preferentially
234 expressed in neurons that are driven by bottom-up visual input.

235 **DISCUSSION**

236 It is well established that both neuronal activity and plasticity are linked to the expression of immediate
237 early genes (Dudek, 2008; Mahringer et al., 2019; Minatohara et al., 2015; Wang et al., 2021; Yap and
238 Greenberg, 2018). Comparably little, however, is known about how specific functional characteristics of
239 neurons relate to the expression of immediate early genes. Here we investigated the relationship
240 between the expression of three IEGs (Arc, c-Fos, and EGR1) and functional responses in excitatory layer
241 2/3 neurons of mouse visual cortex. We found that during visuomotor learning following a mouse's first
242 visual exposure in life, Arc was preferentially expressed in neurons that are driven by excitatory bottom-
243 up visual input, while EGR1 was preferentially expressed in neurons that are driven by motor-related
244 input. In addition, we found that neurons expressing high levels of EGR1 exhibit visuomotor mismatch
245 responses higher than the rest of the population, while neurons expressing high levels of Arc exhibit
246 visuomotor mismatch responses weaker than the rest of the population.

247 Such a relationship between a neuron's IEG expression profile and its functional properties could be
248 explained by differences in the contribution of different IEGs to different types of input synapses. Arc, c-

249 Fos, and EGR1 all have unique cellular functions, and it is conceivable that they make different
250 contributions to different synapse types. Genes for a subset of GABA_A receptor subunits, for example,
251 are transcriptional targets of EGR1 (Mo et al., 2015). If the postsynaptic subunit composition of the
252 GABA receptor is correlated with the presynaptic inhibitory cell type, EGR1 expression could
253 preferentially upregulate specific inhibitory input pathways. Similar input pathway-specific roles have
254 been described for other IEGs. Neuronal activity-regulated pentraxin (NARP) is secreted by pyramidal
255 neurons and exclusively accumulates at parvalbumin-positive inhibitory neurons where it regulates
256 excitatory synapses onto these cells (Chang et al., 2010; Gu et al., 2013). The activity-dependent
257 transcription factor NPAS4 has been found to restrict the number of synapses of mossy-fiber input
258 specifically onto CA3 pyramidal cells during learning (Weng et al., 2018).

259 Our data would be consistent with the interpretation that the IEG expression pattern of a given neuron
260 correlates with its pattern of synaptic inputs. Neurons that predominantly receive excitatory bottom-up
261 drive likely require a different distribution and type of input synapses compared to neurons that receive
262 mainly top-down excitatory drive. Layer 2/3 neurons that exhibit strong motor-related and mismatch
263 responses are thought to be driven by top-down excitatory inputs (Leinweber et al., 2017), which
264 predominantly target apical dendrites (Petreanu et al., 2009). Conversely, layer 2/3 neurons with strong
265 visual responses are thought to be driven by bottom-up visual inputs, which predominantly target basal
266 dendrites (Petreanu et al., 2009). We have speculated that mismatch neurons that receive motor-
267 related input also receive matched bottom-up inhibitory input from a specific subset of somatostatin
268 (SST)-positive interneurons (Attinger et al., 2017). Thus, EGR1 expression may be preferentially
269 increased in neurons that are driven by excitatory top-down input and SST mediated bottom-up
270 inhibition, while Arc expression may be preferentially increased in neurons that are driven by excitatory
271 bottom-up visual input. This may explain why a change to the visual input alone at first visual exposure
272 primarily resulted in a rearrangement of the Arc expression pattern (**Figure 2D**) but left the EGR1
273 expression pattern relatively unaffected (**Figure 2F**), while first exposure to normal visuomotor coupling
274 resulted in a rearrangement of the expression pattern of both Arc and EGR1. It is also consistent with
275 the fact that experience dependent changes of EGR1 expression are primarily observed in superficial
276 layer 2/3 neurons (Xie et al., 2014) that likely are more strongly targeted by top-down input than deep
277 layer 2/3 neurons.

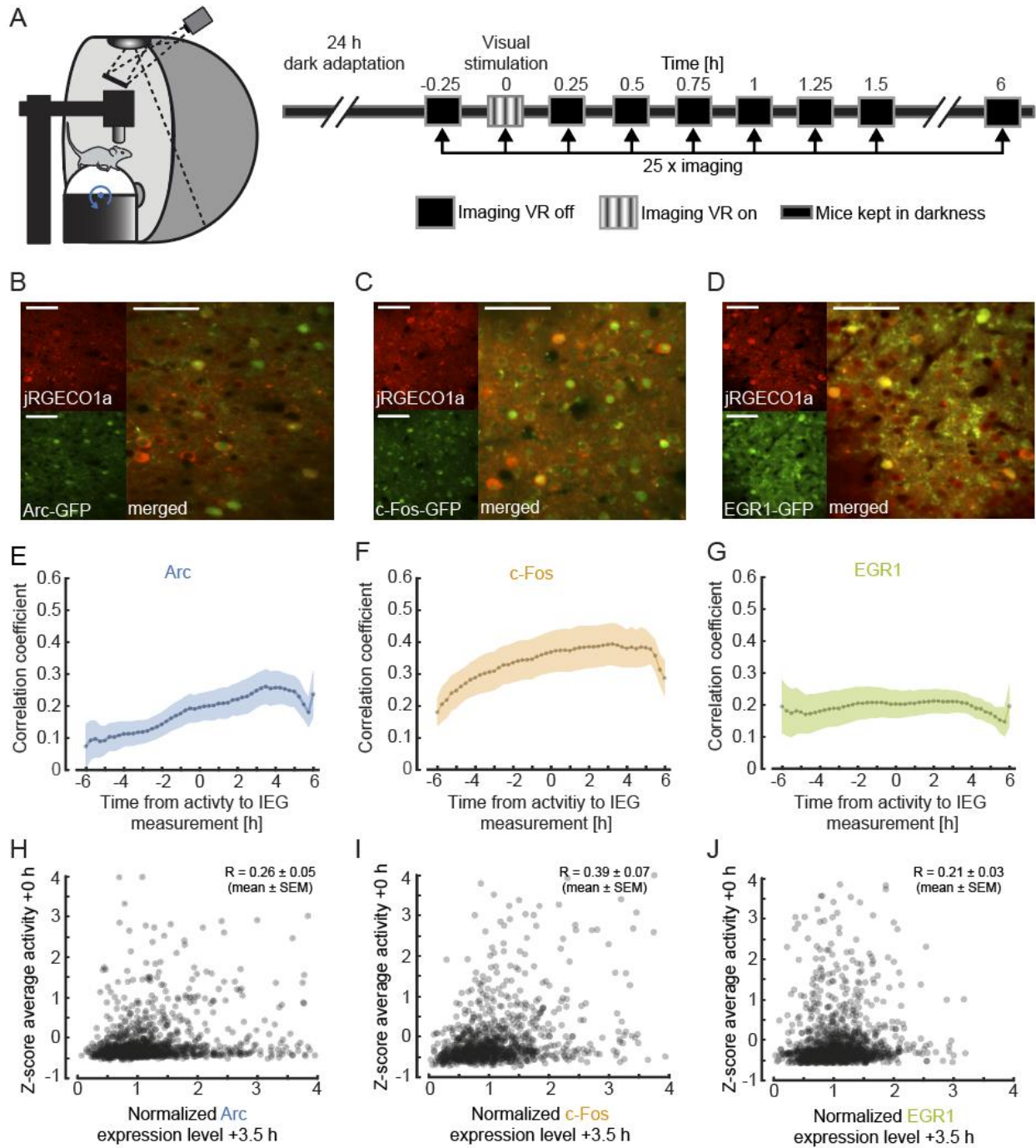
278 When interpreting our results, it should be kept in mind that both the method we use to approximate
279 IEG expression levels and the method we use to approximate neuronal activity levels come with a series

280 of caveats. In the case of the transgenic mice used for the IEG expression measurements, two of these
281 express a fusion protein (Arc and c-Fos), where the IEG is likely overexpressed (Steward et al., 2017), and
282 it is possible that the decay kinetics of the fusion protein differ from those of the native protein. In the
283 case of the GFP driven by the *egr1* promoter, the GFP decay kinetics are likely different from the decay
284 kinetics of EGR1. However, these potential differences in decay kinetics and expression levels do not
285 completely mask the correlation between IEG expression levels and reporter proteins. In post-mortem
286 histological stainings the expression of GFP in these mouse lines overlaps well with the expression levels
287 of the IEGs (Barth et al., 2004; Okuno et al., 2012; Wang et al., 2021; Xie et al., 2014; Yassin et al., 2010).
288 Thus, reporter protein levels reflect a filtered version of IEG expression levels, and the two are likely
289 related by a monotonic function. Given that all our analyses rely only on relative expression levels
290 among populations of simultaneously recorded neurons or relative changes of expression levels in time,
291 the lack of a direct measurement of IEG expression levels should not change our conclusions. A second
292 caveat concerns the genetically encoded calcium indicator used to measure neuronal activity. Our
293 activity measures are biased towards bursts of neuronal activity, as single spikes are probably not always
294 detectable using calcium indicators *in vivo*. However, even though the transfer function from neuronal
295 activity to calcium signal is non-linear, it is monotonic. Thus, we may be underestimating the correlation
296 between neuronal activity and IEG expression, but neither caveat would bias the results towards finding
297 specific correlations between different IEGs and functional cell types. Lastly, to experimentally separate
298 first visual exposure from first visuomotor exposure, and to be able to record neuronal activity
299 throughout this paradigm, we had to dark rear mice from birth. Dark rearing is known to delay normal
300 development of V1 (Hensch, 2005; Sherman and Spear, 1982). However, using a similar experimental
301 paradigm, we have previously found that dark rearing did not impair development of visuomotor
302 integration once mice are exposed to normal visuomotor coupling (Attinger et al., 2017). Thus, given
303 that our conclusions are based on differences between different groups of mice that were all dark
304 reared, the caveats associated with the dark rearing are unlikely to substantially alter our conclusions.

305 In summary, our results suggest that the expression of Arc and EGR1 in layer 2/3 neurons in mouse
306 visual cortex may be a correlate of the type of functional input the neuron receives. Such a preference
307 for expression in a functionally specific subset of neurons would be consistent with differential changes
308 in the ratio of the expression of different IEGs under conditions that result in identical mean levels of
309 neuronal activity (Bailey and Wade, 2003; Farina and Commins, 2016; Guzowski et al., 2006) that are
310 difficult to explain if IEG expression were simply driven by mean activity. In future experiments, it will be

311 important to establish a more detailed picture of how immediate early genes could orchestrate or
312 stabilize the pattern of functionally distinct input streams a neuron receives.

313 FIGURES



314

315 **Figure 1. Simultaneous imaging of neuronal activity and immediate early gene expression in visual**
316 **cortex.**

317 **(A)** Left: Schematic of the virtual reality setup used for imaging experiments. Right: Schematic of the
318 experimental timeline. Mice were dark-adapted for 24 hours. Neuronal activity and IEG expression levels
319 were recorded in 25 imaging sessions starting immediately before and continuing until 6 hours after
320 visual stimulation in intervals of 15 minutes.

321 **(B)** Example two-photon images of neurons in primary visual cortex labelled with jRGECO1a (red, top
322 left), Arc (green, bottom left), and the overlay (right). Scale bar is 50 μm .

323 **(C)** Same as in **(B)**, but for c-Fos.

324 **(D)** Same as in **(B)**, but for EGR1.

325 **(E)** Correlation of average activity and IEG expression level as a function of the time difference between
326 the two measurements. Positive values correspond to activity measurement that preceded the IEG
327 measurement. Dotted line indicates average correlation, shading indicates standard error of the mean
328 (SEM) across mice ($n = 4$).

329 **(F)** Same as in **(E)**, but for c-Fos mice ($n = 4$).

330 **(G)** Same as in **(E)**, but for EGR1 mice ($n = 4$).

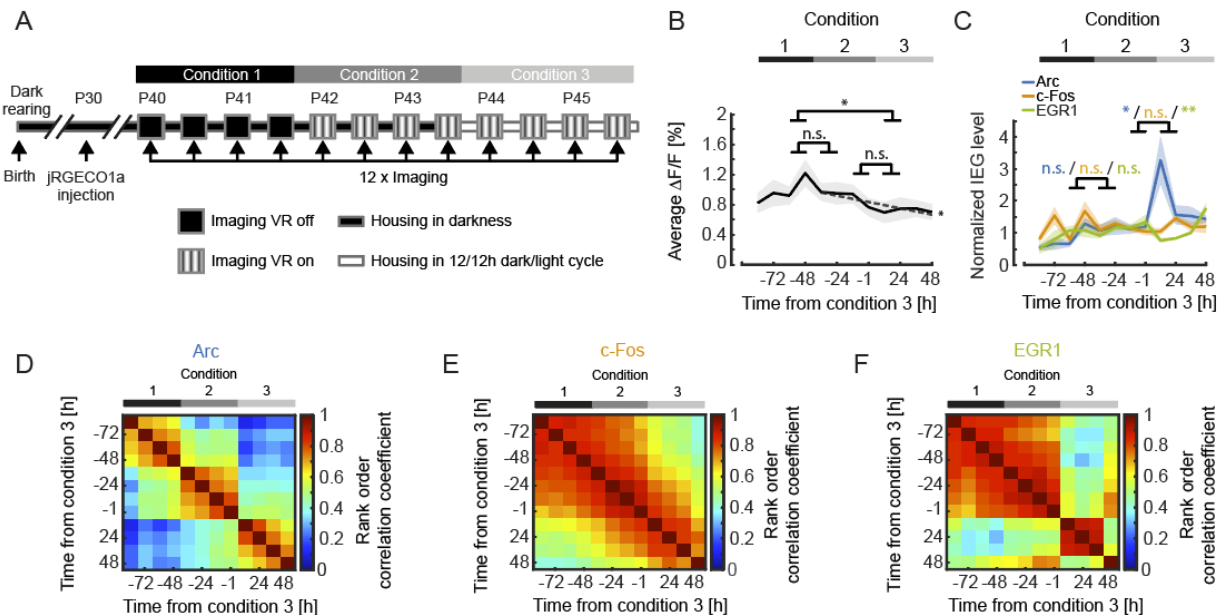
331 **(H)** Scatter plot of Arc expression 3.5 hours after visual stimulation and average neuronal activity during
332 visual stimulation (1382 neurons in 4 mice, 83 neurons outside of plot range). Shown in the panel is the
333 average correlation coefficient across mice (mean \pm SEM, $n = 4$).

334 **(I)** Same as in **(H)**, but for c-Fos (1070 neurons in 4 mice, 28 neurons outside of plot range).

335 **(J)** Same as **(H)**, but for EGR1 (1319 neurons in 4 mice, 18 neurons outside of plot range).

336

337



338

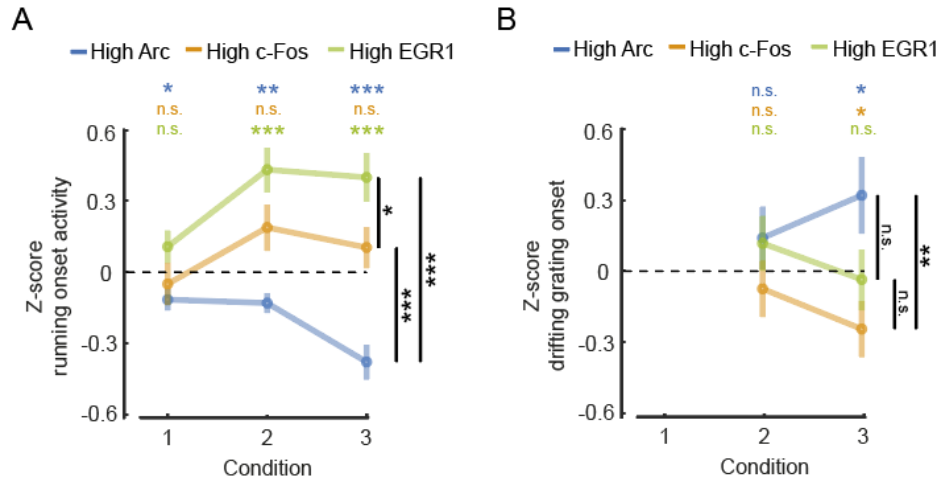
339 **Figure 2. IEG expression dynamics during visuomotor learning.**

340 (A) Schematic of the experimental timeline. Mice were born and reared in complete darkness. jRGECO1a
 341 was injected 10 to 12 days prior to the start of imaging experiments. We then imaged calcium activity
 342 and IEG expression levels every 12 h over the course of 6 days both before and after first visual exposure
 343 and first exposure to normal visuomotor coupling. On the first two days (condition 1) activity in visual
 344 cortex was recorded in complete darkness while mice were head-fixed and free to run on a spherical
 345 treadmill. On the third day of recording mice were exposed to visual feedback (first visual exposure) in a
 346 virtual reality environment. Outside of the recording sessions mice were still housed in complete
 347 darkness (condition 2). Starting on day 5, mice were subjected to a 12 h / 12 h light/dark cycle (condition
 348 3).

349 (B) Average calcium activity during all conditions (condition 1 vs. 2: $p = 0.2183$, condition 2 vs. 3: $p =$
 350 0.527 , condition 1 vs. 3: $p = 0.0123$, 5067 neurons, paired t-test). Shading is SEM over mice. Dashed line
 351 indicates linear fit to the data of conditions 2 and 3. The linear fit to the data from conditions 2 and 3
 352 exhibited a significant negative slope ($p = 0.0293$, $R^2 = 0.371$, linear trend analysis, see Methods).

353 (C) Normalized mean IEG expression levels during all conditions. Expression level of Arc (blue, 1969
 354 neurons in 7 mice) significantly increased after first exposure to visuomotor coupling, decreased for
 355 EGR1 (green, 1213 neurons in 4 mice) and remained unchanged for c-Fos (orange, 1885 neurons in 5
 356 mice). Change in IEG expression level between conditions 1 and 2 for Arc: 0.1764 ± 0.1556 , $p = 0.2775$; c-
 357 Fos: -0.0536 ± 0.1877 , $p = 0.7816$; EGR1: -0.0371 ± 0.1246 , $p = 0.7745$ (mean \pm SEM, paired t-test).
 358 Change in IEG expression level between conditions 2 and 3 for Arc: 1.2628 ± 0.5012 , $p = 0.0256$; c-Fos:
 359 0.01612 ± 0.1372 , $p = 0.2702$; EGR1: -0.4568 ± 0.1130 , $p = 0.0049$ (mean \pm SEM, t-test). Shading
 360 indicates SEM over mice.

- 361 **(D)** Average rank order correlation coefficients for Arc expression during visuomotor learning (7 mice).
362 The expression pattern changes both at the onset of conditions 2 and 3.
- 363 **(E)** Same as in **(D)**, but for c-Fos (5 mice). The expression pattern exhibits no apparent transitions.
- 364 **(F)** Same as in **(D)**, but for EGR1 (4 mice). The expression pattern changes at the onset of condition 3.
- 365



366

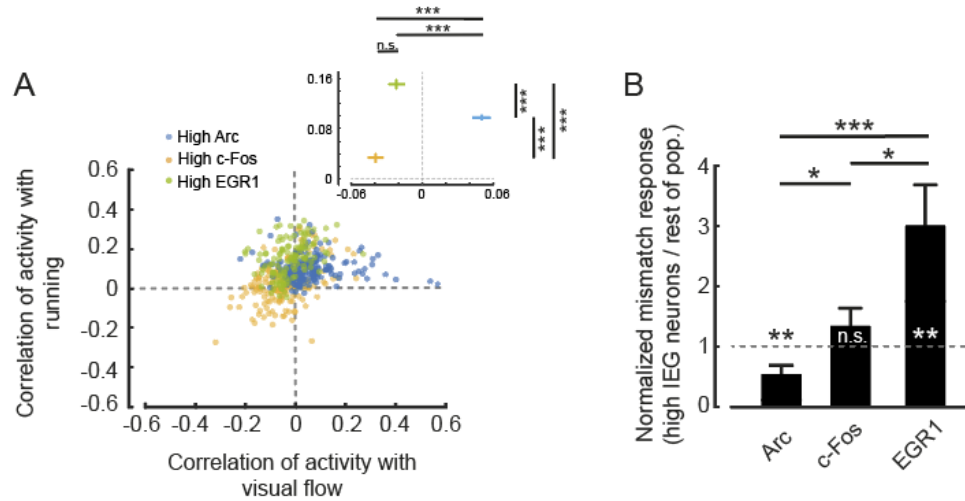
367 **Figure 3. Differential relationship between IEG expression and motor-related and visual responses.**

368 **(A)** Average running onset response during darkness for the top 10 % IEG expressing neurons (Arc: 197
 369 neurons, c-Fos: 189 neurons, EGR1: 121 neurons). Neuronal responses were pooled from all
 370 experimental sessions for each condition, subtracted by the mean and normalized by the standard
 371 deviation of the response of all neurons (Z-score). Error bars are SEM over neurons. Statistics above the
 372 plot indicate comparisons against 0, statistics to the right are between-group comparisons. n.s.: $p > 0.05$,
 373 *: $p < 0.05$, **: $p < 0.01$, *** $p < 0.001$, t-test.

374 **(B)** Average grating onset response for the top 10 % IEG expressing neurons (Arc: $n = 197$, c-Fos: $n = 189$,
 375 EGR1: $n = 121$). Neuronal responses were pooled from all experimental sessions for conditions 2 and 3,
 376 subtracted by the mean and normalized by standard deviation of the response of all neurons (Z-score).
 377 Error bars are SEM over neurons. Statistics above the plot indicate comparisons against 0, statistics to
 378 the right are between-group comparisons. n.s.: $p > 0.05$, *: $p < 0.05$, **: $p < 0.01$, *** $p < 0.001$, t-test.

379

380



381

382 **Figure 4. Functional cell type specific expression of IEGs in visual cortex.**

383 **(A)** Correlation of neuronal activity with running and of neuronal activity with visual flow during open-
 384 loop phases of conditions 2 and 3 for the top 10 % IEG expressing neurons (Arc: 197 neurons, c-Fos: 189
 385 neurons, EGR1: 121 neurons). Inset: Average correlation coefficient for the three groups of high IEG
 386 expressing neurons. High Arc expressing neurons had the highest correlation with visual flow (Arc vs. c-
 387 Fos: $p < 10^{-10}$, Arc vs. EGR1: $p < 10^{-9}$, c-Fos vs. EGR1: $p = 0.0791$, t-test), while high EGR1 expressing
 388 neurons had the highest correlation with running (Arc vs. c-Fos: $p < 10^{-10}$, Arc vs. EGR1: $p < 10^{-8}$, c-Fos vs.
 389 EGR1: $p < 10^{-10}$, t-test).

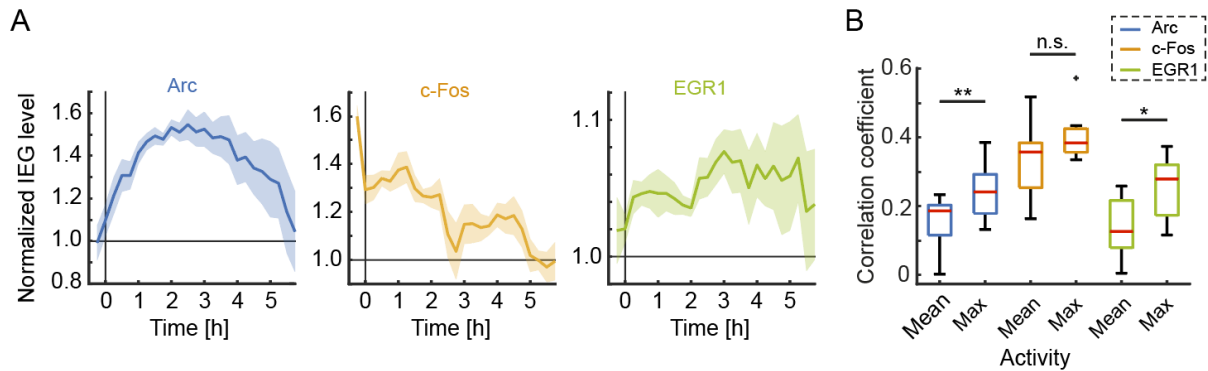
390 **(B)** Mismatch responses in condition 3 were significantly higher for the top 10 % EGR1 expressing
 391 neurons and significantly lower for the top 10 % Arc expressing neurons than the rest of the respective
 392 population (Arc: 197 neurons, c-Fos: 189 neurons, EGR1: 121 neurons). Arc: $p = 0.0461$, c-Fos: $p =$
 393 0.2273 , EGR1: $p = 0.0234$; Arc vs. c-Fos: $p = 0.0101$, c-Fos vs. EGR1: $p = 0.048$, Arc vs. EGR1: $p = 0.0057$, t-
 394 test.

395

396

397 **Supplementary Figures**

398



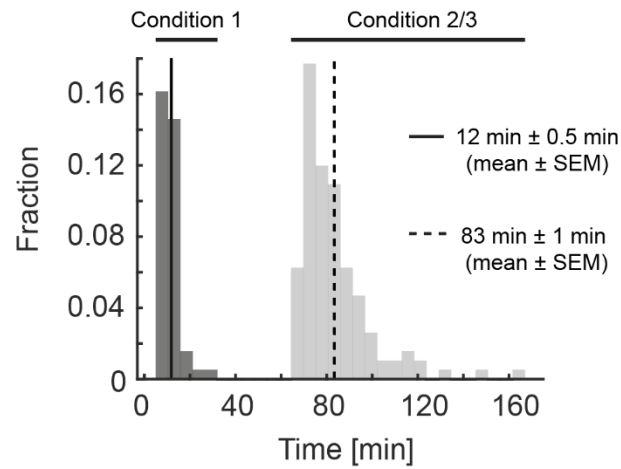
399

400 **Figure S1. Time course of IEG expression during the imaging paradigm and correlation of IEG**
401 **expression with mean and maximum neuronal activity. Related to Figure 1.**

402 (A) Time course of normalized IEG expression levels following 24 h dark adaptation and 15 min visual
403 stimulation at time 0. Shading indicates SEM over neurons.

404 (B) Correlation coefficient of mean and maximum activity (average across or peak within a recording
405 session, respectively) with IEG expression 3.5 h after stimulation or recording onset (Arc: 11 mice, c-Fos:
406 9 mice, EGR1: 8 mice). Box whisker plot: red line indicates median, box marks 25th to 75th percentiles
407 and whiskers extended to the next most extreme datapoint within a range of 1.5 times the interquartile
408 distance (rank sum test, Arc: $p = 0.0086$, c-Fos: $p = 0.1359$, EGR1: $p = 0.0207$).

409



410

411 **Figure S2. Duration of recording sessions. Related to Figure 2.**

412 Histogram of the durations of the recording sessions. On average, one recording session lasted for
413 approximately 12 min during condition 1 (solid line) and, due to the addition of closed-loop, open-loop,
414 and grating stimulation phases, 83 min during conditions 2 and 3 (dashed line).

415

416 METHODS

417 **Animals and surgery.** All animal procedures were approved by and carried out in accordance with
418 guidelines of the Veterinary Department of the Canton Basel-Stadt, Switzerland. We used imaging data
419 from a total of 11 EGFP-Arc mice (Okuno et al., 2012), 9 c-Fos-GFP mice (Barth et al., 2004) and 8 EGR1-
420 GFP mice (Xie et al., 2014), aged 40 days at the start of visuomotor learning (**Figures 2 - 4**) or aged 100-
421 104 (Arc), 279-291 (c-Fos) or 120-124 (EGR1) days (**Figure 1**). Sample sizes were chosen according to the
422 standards in the field and no statistical methods were used to predetermine sample sizes. Mice were
423 group-housed in a dark cabinet and in a vivarium (light/dark cycle: 12 h / 12 h). Viral injections and
424 window implantation were performed as previously described (Dombeck et al., 2010; Leinweber et al.,
425 2014). Briefly, for sensorimotor learning experiments, mice (aged 29 d \pm 1 d, mean \pm SEM) were
426 anesthetized in darkness using a mix of fentanyl (0.05 mg/kg), medetomidine (0.5 mg/kg) and
427 midazolam (5 mg/kg), and additionally their eyes were covered with a thick, black cotton fabric during
428 all surgical procedures. A 3 mm to 5 mm craniotomy was made above visual cortex (2.5 mm lateral of
429 lambda (Paxinos and Franklin, 2013)) and AAV2/1-Ef1a-NES-jRGECO1a-WPRE ((Dana et al., 2016); titer:
430 between 7.2×10^{10} GC/ml and 6.8×10^{12} GC/ml) was injected into the target region. The craniotomy was
431 sealed with a fitting cover slip. A titanium head bar was attached to the skull and stabilized with dental
432 cement.

433 **Imaging and virtual reality.** Imaging commenced 10 – 12 (visuomotor learning experiments, **Figures 2 -**
434 **4**) or 12 – 29 (**Figure 1**) days following virus injection and was carried out using a custom-built two-
435 photon microscope. Illumination source was a Chameleon Vision laser (Coherent) tuned to a wavelength
436 of either 950 nm, 990 nm or 1030 nm. Imaging was performed using an 8 kHz resonance scanner
437 (Cambridge Technology) resulting in frame rates of 40 Hz at a resolution of 400×750 pixels. In addition,
438 we used a piezo actuator (Physik Instrumente) to move the objective (Nikon 16x, 0.8 NA) in steps of 15
439 μm between frames to acquire images at four different depths, thus reducing the effective frame rate to
440 10 Hz. The behavioral imaging setup was as previously described (Leinweber et al., 2014). After brief
441 isoflurane anesthesia mice were head-fixed in complete darkness and the setup was light-shielded
442 before every imaging session. Mice were free to run on an air-supported polystyrene ball, the motion of
443 which was restricted to the forward and backward directions by a pin. The ball's rotation was coupled to
444 linear displacement in the virtual environment that was projected onto a toroidal screen surrounding
445 the mouse. The screen covered a visual field of approximately 240 degrees horizontally and 100 degrees
446 vertically. All displayed elements of the tunnel or sinusoidal gratings were calibrated to be isoluminant.

447 **Experimental design.** For experiments shown in **Figure 1**, mice were dark-adapted for 24 h and 17 min ±
448 10 min (mean ± SEM, 12 mice) before head fixation under the microscope in darkness. Activity and
449 immediate early gene expression were recorded every 15 minutes for 6 hours. Except for the time of
450 visual stimulation with sinusoidal gratings moving in 8 different directions (a total of 80 presentation in
451 random order), mice were kept in complete darkness under the microscope for the duration of the
452 entire experiment. For visuomotor learning experiments (**Figures 2 - 4**) mice were born and reared in
453 complete darkness until P44 and then transferred to a vivarium with a 12 h /12 h light/dark cycle.
454 Experimental sessions started on P40 and occurred twice per day, spaced 12 h apart. In condition 1, all
455 imaging was done in complete darkness and experiments consisted of recording approximately 8 min of
456 neuronal activity during which mice were free to run on the spherical treadmill. IEG expression level
457 measurements were taken before and after each activity recording. In conditions 2 and 3, neuronal
458 activity measurements consisted of 7 recordings of approximately 8 minutes each. Each recording
459 session started with a recording in darkness, followed by a closed-loop recording. In the closed-loop
460 recording, the movement of the mouse in a linear virtual corridor (sinusoidal vertical grating) was
461 coupled to the locomotion of the mouse on the spherical treadmill. During the closed-loop session we
462 included brief (1 s) halts of visual flow to induce mismatch events (Attinger et al., 2017). The subsequent
463 two recordings were of the open-loop type and consisted of a playback of the visual flow the mouse had
464 generated during the preceding closed-loop recording. Subsequently, mice were exposed to a second
465 recording in darkness, followed by a visual stimulation recording. During the visual stimulation
466 sinusoidal moving grating stimuli (2 second standing grating, 3 second drifting grating, 8 different
467 orientations, 10 presentations of each orientation, in a randomized order) were presented. Finally, mice
468 were exposed to a third recording in darkness. In early phases of the experiment mice were encouraged
469 to run by applying occasional mild air puffs to the neck.

470 **Data analysis.** Imaging data were full-frame registered using a custom-written software (Leinweber et
471 al., 2014). Neurons were selected manually based on their mean fluorescence or maximum projection in
472 the red channel (jRGECO1a). This biased our selection towards active neurons. Fluorescence traces were
473 calculated as the mean pixel value in each region of interest per frame, and were then median-
474 normalized to calculate $\Delta F/F$. $\Delta F/F$ traces were filtered as previously described (Dombeck et al., 2007).
475 GFP intensities were calculated as the mean pixel value in each region of interest (ROI) for mean
476 fluorescence projections. To compensate for expression level differences between different IEG mouse
477 lines as well as for image quality differences between different mice we normalized the GFP level

478 measurements as follows: For each mouse, all ROI measurements were subtracted by the minimum
479 calculated over all ROIs and timepoints, and normalized by the median over all ROIs and timepoints.

$$480 \quad ROI_{normalized}^{i,tp} = (ROI^{i,tp} - \min_{i,tp} ROI^{i,tp}) / (\text{median}_{i,tp} ROI^{i,tp} - \min_{i,tp} ROI^{i,tp})$$

481 This ensured that the minimum value of IEG expression was 0 and the median 1. No blinding of
482 experimental condition was performed in any of the analyses. Statistical tests were used as stated in the
483 figure legends.

484 **Figure 1.** Examples images (**Figures 1B-1D**) are average projections of the recorded channel. IEG
485 expression was normalized as described above (**Figures 1E-1G**). Correlation coefficients (**Figures 1E-1G**)
486 were calculated based on the neuronal population vectors of average activity and IEG expression per
487 measurement timepoint, for each mouse. For the statistical comparison of the correlation coefficients of
488 IEG expression levels with neural activity between the three different groups (4 mice per group), data
489 were bootstrapped 5 times with random replacement and then a t-test was performed on the
490 bootstrapped data.

491 **Figure 2.** To compare changes in neural activity and IEG expression levels between conditions we
492 averaged data from the last two recording sessions of the previous condition and the first two recording
493 sessions of the following condition (**Figures 2B and 2C**). Linear trend analysis (**Figure 2B**) was performed
494 using the MATLAB regress function treating the average activity per timepoint for each mouse as an
495 independent observation. To quantify the significance of the linear trend we report the R^2 statistic and
496 p-value of the F statistic. The linear fit shown (**Figure 2B**), is the average over the linear fits performed to
497 the data of each mouse individually using the MATLAB polyfit and polyval functions. Rank order
498 correlation coefficients (**Figures 2D-2F**) were determined based on the population vectors of average
499 IEG expression per measurement timepoint and mouse, and then averaged.

500 **Figure 3.** For plots of event-triggered activity changes $\Delta F/F$ traces were baseline-subtracted by the
501 average $\Delta F/F$ in a window -500 ms to -100 ms preceding the event onset. Z-scores were obtained on a
502 population vector with average stimulus onset values calculated over a response window of 1.5 s. High
503 IEGs neurons were selected as the top 10% of IEG expressing neurons based on average expression level
504 on the first day of condition 3.

505 **Figure 4.** Correlation coefficients (**Figure 4A**) were calculated by correlating each neuron's activity trace
506 with either the running trace or the visual flow trace during open-loop phases. High IEG neurons were

507 selected with the same criteria used for **Figure 3**. Stimulus-triggered fluorescence changes (**Figure 4B**)
508 were mean-subtracted in a window -500 ms to -100 ms preceding the stimulus onset. Responses were
509 quantified in a window of 1.5 s.

510 **Figure S1**. Correlation coefficients of mean or maximum activity with IEG expression were calculated for
511 each mouse (**Figure S1B**). Mice from visual stimulation experiments (**Figure 1**) and sensorimotor learning
512 experiments (**Figures 2-4**) were pooled for this analysis. For mice from the sensorimotor learning
513 experiments the calculation was done using mean or maximum activity of the first recording segment
514 and the last IEG measurement within a session. Shown is the average correlation across all sessions.

515 **Code and data availability**. All imaging and image processing code can be found online at
516 <https://sourceforge.net/projects/iris-scanning/> (IRIS, imaging software package) and
517 <https://sourceforge.net/p/iris-scanning/calliope/HEAD/tree> (Calliope, image processing software
518 package). All the raw data and analysis code used in this study can be downloaded from the following
519 website: <http://data.fmi.ch/PublicationSupplementRepo/>.

520

521 **ACKNOWLEDGEMENTS**

522 We thank the entire Keller lab for helpful discussion and comments on earlier versions of this
523 manuscript. We thank Daniela Gerosa-Erni for production of the AAV vectors. This work was supported
524 by the Swiss National Science Foundation (GBK), the Novartis Research Foundation (GBK), the Human
525 Frontier Science Program (GBK), and JSPS-Kakenhi and AMED (HO and HB).

526

527 **AUTHOR CONTRIBUTIONS**

528 D.M. and P.Z. performed the experiments, D.M. analyzed the data. H.O. and H.B. made the EGFP-Arc
529 mouse. All authors wrote the manuscript.

530 **REFERENCES**

- 531 Attinger, A., Wang, B., and Keller, G.B. (2017). Visuomotor Coupling Shapes the Functional Development
532 of Mouse Visual Cortex. *Cell* *169*, 1291-1302.e14.
- 533 Bailey, D.J., and Wade, J. (2003). Differential expression of the immediate early genes FOS and ZENK
534 following auditory stimulation in the juvenile male and female zebra finch. *Brain Research. Molecular*
535 *Brain Research* *116*, 147–154.
- 536 Barth, A.L., Gerkin, R.C., and Dean, K.L. (2004). Alteration of Neuronal Firing Properties after In Vivo
537 Experience in a FosGFP Transgenic Mouse. *The Journal of Neuroscience* *24*, 6466–6475.
- 538 Bozon, B., Kelly, A., Josselyn, S.A., Silva, A.J., Davis, S., and Laroche, S. (2003). MAPK, CREB and zif268 are
539 all required for the consolidation of recognition memory. *Philosophical Transactions of the Royal Society*
540 *of London. Series B, Biological Sciences* *358*, 805–814.
- 541 Bullitt, E. (1990). Expression of C-fos-like protein as a marker for neuronal activity following noxious
542 stimulation in the rat. *The Journal of Comparative Neurology* *296*, 517–530.
- 543 Chang, M.C., Park, J.M., Pelkey, K.A., Grabenstatter, H.L., Xu, D., Linden, D.J., Sutula, T.P., McBain, C.J.,
544 and Worley, P.F. (2010). Narp regulates homeostatic scaling of excitatory synapses on parvalbumin-
545 expressing interneurons. *Nat Neurosci* *13*, 1090–1097.
- 546 Chowdhury, S., Shepherd, J.D., Okuno, H., Lyford, G., Petralia, R.S., Plath, N., Kuhl, D., Huganir, R.L., and
547 Worley, P.F. (2006). Arc/Arg3.1 Interacts with the Endocytic Machinery to Regulate AMPA Receptor
548 Trafficking. *Neuron* *52*, 445–459.
- 549 Dana, H., Mohar, B., Sun, Y., Narayan, S., Gordus, A., Hasseman, J.P., Tsegaye, G., Holt, G.T., Hu, A.,
550 Walpita, D., et al. (2016). Sensitive red protein calcium indicators for imaging neural activity. *ELife* *5*.
- 551 Denny, C.A., Kheirbek, M.A., Alba, E.L., Tanaka, K.F., Brachman, R.A., Laughman, K.B., Tomm, N.K., Turi,
552 G.F., Losonczy, A., and Hen, R. (2014). Hippocampal Memory Traces Are Differentially Modulated by
553 Experience, Time, and Adult Neurogenesis. *Neuron* *83*, 189–201.
- 554 Dombeck, D.A., Khabbaz, A.N., Collman, F., Adelman, T.L., and Tank, D.W. (2007). Imaging Large-Scale
555 Neural Activity with Cellular Resolution in Awake, Mobile Mice. *Neuron* *56*, 43–57.
- 556 Dombeck, D.A., Harvey, C.D., Tian, L., Looger, L.L., and Tank, D.W. (2010). Functional imaging of
557 hippocampal place cells at cellular resolution during virtual navigation. *Nature Neuroscience* *13*, 1433–
558 1440.
- 559 Dudek, S. (2008). *Transcriptional Regulation by Neuronal Activity* (Boston, MA: Springer US).
- 560 Farina, F.R., and Commins, S. (2016). Differential expression of immediate early genes Zif268 and c-Fos
561 in the hippocampus and prefrontal cortex following spatial learning and glutamate receptor antagonism.
562 *Behavioural Brain Research* *307*, 194–198.
- 563 Fiser, J., Chiu, C., and Weliky, M. (2004). Small modulation of ongoing cortical dynamics by sensory input
564 during natural vision. *Nature* *431*, 573–578.

- 565 Fleischmann, A., Hvalby, O., Jensen, V., Strekalova, T., Zacher, C., Layer, L.E., Kvello, A., Reschke, M.,
566 Spanagel, R., Sprengel, R., et al. (2003). Impaired Long-Term Memory and NR2A-Type NMDA Receptor-
567 Dependent Synaptic Plasticity in Mice Lacking c-Fos in the CNS. *The Journal of Neuroscience* *23*, 9116–
568 9122.
- 569 Gandolfi, D., Cerri, S., Mapelli, J., Polimeni, M., Tritto, S., Fuzzati-Armentero, M.-T., Bigiani, A., Blandini,
570 F., Mapelli, L., and D’Angelo, E. (2017). Activation of the CREB/c-FosPathway during Long-Term Synaptic
571 Plasticity in the Cerebellum Granular Layer. *Frontiers in Cellular Neuroscience* *11*, 184.
- 572 Gao, M., Sossa, K., Song, L., Errington, L., Cummings, L., Hwang, H., Kuhl, D., Worley, P., and Lee, H.-K.
573 (2010). A Specific Requirement of Arc/Arg3.1 for Visual Experience-Induced Homeostatic Synaptic
574 Plasticity in Mouse Primary Visual Cortex. *The Journal of Neuroscience* *30*, 7168–7178.
- 575 Garner, A.R., Rowland, D.C., Hwang, S.Y., Baumgaertel, K., Roth, B.L., Kentros, C., and Mayford, M.
576 (2012). Generation of a Synthetic Memory Trace. *Science (New York, N.Y.)* *335*, 1513–1516.
- 577 Greenberg, M.E., and Ziff, E.B. (1984). Stimulation of 3T3 cells induces transcription of the c-fos proto-
578 oncogene. *Nature* *311*, 433–438.
- 579 Gu, Y., Huang, S., Chang, M.C., Worley, P., Kirkwood, A., and Quinlan, E.M. (2013). Obligatory Role for
580 the Immediate Early Gene NARP in Critical Period Plasticity. *Neuron* *79*, 335–346.
- 581 Guzowski, J.F. (2002). Insights into immediate-early gene function in hippocampal memory consolidation
582 using antisense oligonucleotide and fluorescent imaging approaches. *Hippocampus* *12*, 86–104.
- 583 Guzowski, J.F., and McGaugh, J.L. (1997). Antisense oligodeoxynucleotide-mediated disruption of
584 hippocampal cAMP response element binding protein levels impairs consolidation of memory for water
585 maze training. *Proceedings of the National Academy of Sciences of the United States of America* *94*,
586 2693–2698.
- 587 Guzowski, J.F., McNaughton, B.L., Barnes, C.A., and Worley, P.F. (1999). Environment-specific expression
588 of the immediate-early gene Arc in hippocampal neuronal ensembles. *Nature Neuroscience* *2*, 1120–
589 1124.
- 590 Guzowski, J.F., Lyford, G.L., Stevenson, G.D., Houston, F.P., McGaugh, J.L., Worley, P.F., and Barnes, C. a
591 (2000). Inhibition of activity-dependent arc protein expression in the rat hippocampus impairs the
592 maintenance of long-term potentiation and the consolidation of long-term memory. *The Journal of*
593 *Neuroscience : The Official Journal of the Society for Neuroscience* *20*, 3993–4001.
- 594 Guzowski, J.F., Miyashita, T., Chawla, M.K., Sanderson, J., Maes, L.I., Houston, F.P., Lipa, P., McNaughton,
595 B.L., Worley, P.F., and Barnes, C.A. (2006). Recent behavioral history modifies coupling between cell
596 activity and Arc gene transcription in hippocampal CA1 neurons. *Proceedings of the National Academy*
597 *of Sciences of the United States of America* *103*, 1077–1082.
- 598 Hengen, K.B., Torrado Pacheco, A., McGregor, J.N., Van Hooser, S.D., and Turrigiano, G.G. (2016).
599 Neuronal Firing Rate Homeostasis Is Inhibited by Sleep and Promoted by Wake. *Cell* *165*, 180–191.
- 600 Hensch, T.K. (2005). Critical period plasticity in local cortical circuits. *Nature Reviews Neuroscience* *6*,
601 877–888.

- 602 Holtmaat, A., and Caroni, P. (2016). Functional and structural underpinnings of neuronal assembly
603 formation in learning. *Nature Neuroscience* *19*, 1553–1562.
- 604 Jarvis, E.D., Ribeiro, S., Da Silva, M.L., Ventura, D., Vielliard, J., and Mello, C. V. (2000). Behaviourally
605 driven gene expression reveals song nuclei in hummingbird brain. *Nature* *406*, 628–632.
- 606 Jenks, K.R., Kim, T., Pastuzyn, E.D., Okuno, H., Taibi, A. V, Bito, H., Bear, M.F., and Shepherd, J.D. (2017).
607 Arc restores juvenile plasticity in adult mouse visual cortex. *Proceedings of the National Academy of*
608 *Sciences* *114*, 9182–9187.
- 609 Jones, M.W., Errington, M.L., French, P.J., Fine, A., Bliss, T.V.P., Garel, S., Charnay, P., Bozon, B., Laroche,
610 S., and Davis, S. (2001). A requirement for the immediate early gene Zif268 in the expression of late LTP
611 and long-term memories. *Nature Neuroscience* *4*, 289–296.
- 612 Jordan, R., and Keller, G.B. (2020). Opposing Influence of Top-down and Bottom-up Input on Excitatory
613 Layer 2/3 Neurons in Mouse Primary Visual Cortex. *Neuron* *108*, 1194-1206.e5.
- 614 Josselyn, S.A., Köhler, S., and Frankland, P.W. (2015). Finding the engram. *Nature Reviews Neuroscience*
615 *16*, 521–534.
- 616 Kaminska, B., Kaczmarek, L., and Chaudhuri, A. (1996). Visual Stimulation Regulates the Expression of
617 Transcription Factors and Modulates the Composition of AP-1 in Visual Cortex. *Journal of*
618 *Neuroscience* *16*, 3968–3978.
- 619 Kaplan, I. V, Guo, Y., and Mower, G.D. (1996). Immediate early gene expression in cat visual cortex
620 during and after the critical period: differences between EGR-1 and Fos proteins. *Brain Research.*
621 *Molecular Brain Research* *36*, 12–22.
- 622 Kawashima, T., Kitamura, K., Suzuki, K., Nonaka, M., Kamijo, S., Takemoto-Kimura, S., Kano, M., Okuno,
623 H., Ohki, K., and Bito, H. (2013). Functional labeling of neurons and their projections using the synthetic
624 activity-dependent promoter E-SARE. *Nature Methods* *10*, 889–895.
- 625 Keck, T., Keller, G.B., Jacobsen, R.I., Eysel, U.T., Bonhoeffer, T., and Hübener, M. (2013). Synaptic scaling
626 and homeostatic plasticity in the mouse visual cortex in vivo. *Neuron* *80*.
- 627 Keller, G.B., and Mrsic-Flogel, T.D. (2018). Predictive Processing: A Canonical Cortical Computation.
628 *Neuron* *100*, 424–435.
- 629 Keller, G.B., Bonhoeffer, T., and Hübener, M. (2012). Sensorimotor mismatch signals in primary visual
630 cortex of the behaving mouse. *Neuron* *74*, 809–815.
- 631 Knapska, E., and Kaczmarek, L. (2004). A gene for neuronal plasticity in the mammalian brain:
632 Zif268/Egr-1/NGFI-A/Krox-24/TIS8/ZENK? *Progress in Neurobiology* *74*, 183–211.
- 633 Leinweber, M., Zmarz, P., Buchmann, P., Argast, P., Hübener, M., Bonhoeffer, T., and Keller, G.B. (2014).
634 Two-photon calcium imaging in mice navigating a virtual reality environment. *Journal of Visualized*
635 *Experiments : JoVE* e50885.

- 636 Leinweber, M., Ward, D.R., Sobczak, J.M., Attinger, A., and Keller, G.B. (2017). A Sensorimotor Circuit in
637 Mouse Cortex for Visual Flow Predictions. *Neuron* 95, 1420-1432.e5.
- 638 Liu, X., Ramirez, S., Pang, P.T., Puryear, C.B., Govindarajan, A., Deisseroth, K., and Tonegawa, S. (2012).
639 Optogenetic stimulation of a hippocampal engram activates fear memory recall. *Nature* 484, 381–385.
- 640 Mahringer, D., Petersen, A., Fiser, A., Okuno, H., Bito, H., Perrier, J.-F., and Keller, G. (2019). Expression
641 of c-Fos and Arc in hippocampal region CA1 marks neurons that exhibit learning-related activity changes.
642 *BioRxiv* 644526.
- 643 Makino, H., and Komiyama, T. (2015). Learning enhances the relative impact of top-down processing in
644 the visual cortex. *Nature Neuroscience* 18, 1116–1122.
- 645 Mataga, N., Fujishima, S., Condie, B.G., and Hensch, T.K. (2001). Experience-Dependent Plasticity of
646 Mouse Visual Cortex in the Absence of the Neuronal Activity-Dependent Marker *gr1/zif268*. *The*
647 *Journal of Neuroscience* 21, 9724–9732.
- 648 McCurry, C.L., Shepherd, J.D., Tropea, D., Wang, K.H., Bear, M.F., and Sur, M. (2010). Loss of Arc renders
649 the visual cortex impervious to the effects of sensory experience or deprivation. *Nature Neuroscience*
650 13, 450–457.
- 651 Messaoudi, E., Kanhema, T., Soulé, J., Tiron, A., Dageyte, G., da Silva, B., and Bramham, C.R. (2007).
652 Sustained Arc/Arg3.1 synthesis controls long-term potentiation consolidation through regulation of local
653 actin polymerization in the dentate gyrus in vivo. *The Journal of Neuroscience : The Official Journal of*
654 *the Society for Neuroscience* 27, 10445–10455.
- 655 Minatohara, K., Akiyoshi, M., and Okuno, H. (2015). Role of Immediate-Early Genes in Synaptic Plasticity
656 and Neuronal Ensembles Underlying the Memory Trace. *Frontiers in Molecular Neuroscience* 8, 78.
- 657 Mo, J., Kim, C.-H., Lee, D., Sun, W., Lee, H.W., and Kim, H. (2015). Early growth response 1 (Egr-1)
658 directly regulates GABA receptor $\alpha 2$, $\alpha 4$, and θ subunits in the hippocampus. *Journal of Neurochemistry*
659 133, 489–500.
- 660 Morgan, J.I., Cohen, D.R., Hempstead, J.L., and Curran, T. (1987). Mapping patterns of c-fos expression in
661 the central nervous system after seizure. *Science* 237, 192–197.
- 662 Okuno, H., Akashi, K., Ishii, Y., Yagishita-Kyo, N., Suzuki, K., Nonaka, M., Kawashima, T., Fujii, H.,
663 Takemoto-Kimura, S., Abe, M., et al. (2012). Inverse synaptic tagging of inactive synapses via dynamic
664 interaction of Arc/Arg3.1 with CaMKII β . *Cell* 149, 886–898.
- 665 Paxinos, G., and Franklin, K.B.J. (2013). Paxinos and Franklin's the mouse brain in stereotaxic coordinates
666 (Academic Press).
- 667 Petreanu, L., Mao, T., Sternson, S.M., and Svoboda, K. (2009). The subcellular organization of neocortical
668 excitatory connections. *Nature* 457, 1142–1145.
- 669 Ploski, J.E., Pierre, V.J., Smucny, J., Park, K., Monsey, M.S., Overeem, K.A., and Schafe, G.E. (2008). The
670 activity-regulated cytoskeletal-associated protein (Arc/Arg3.1) is required for memory consolidation of
671 pavlovian fear conditioning in the lateral amygdala. *Journal of Neuroscience* 28, 12383–12395.

- 672 Ramirez, S., Liu, X., Lin, P.-A., Suh, J., Pignatelli, M., Redondo, R.L., Ryan, T.J., and Tonegawa, S. (2013).
673 Creating a false memory in the hippocampus. *Science (New York, N.Y.)* *341*, 387–391.
- 674 Ramírez-Amaya, V., Vazdarjanova, A., Mikhael, D., Rosi, S., Worley, P.F., and Barnes, C.A. (2005). Spatial
675 Exploration-Induced Arc mRNA and Protein Expression: Evidence for Selective, Network-Specific
676 Reactivation. *The Journal of Neuroscience* *25*, 1761–1768.
- 677 Reijmers, L.G., Perkins, B.L., Matsuo, N., and Mayford, M. (2007). Localization of a stable neural
678 correlate of associative memory. *Science (New York, N.Y.)* *317*, 1230–1233.
- 679 Rial Verde, E.M., Lee-Osbourne, J., Worley, P.F., Malinow, R., and Cline, H.T. (2006). Increased
680 Expression of the Immediate-Early Gene Arc/Arg3.1 Reduces AMPA Receptor-Mediated Synaptic
681 Transmission. *Neuron* *52*, 461–474.
- 682 Rosen, K.M., McCormack, M.A., Villa-Komaroff, L., and Mower, G.D. (1992). Brief visual experience
683 induces immediate early gene expression in the cat visual cortex. *Proceedings of the National Academy*
684 *of Sciences of the United States of America* *89*, 5437–5441.
- 685 Saleem, A.B., Ayaz, A., Jeffery, K.J., Harris, K.D., and Carandini, M. (2013). Integration of visual motion
686 and locomotion in mouse visual cortex. *Nature Neuroscience* *16*, 1864–1869.
- 687 Shepherd, J.D., and Bear, M.F. (2011). New views of Arc, a master regulator of synaptic plasticity. *Nature*
688 *Neuroscience* *14*, 279–284.
- 689 Shepherd, J.D., Rumbaugh, G., Wu, J., Chowdhury, S., Plath, N., Kuhl, D., Huganir, R.L., and Worley, P.F.
690 (2006). Arc/Arg3.1 Mediates Homeostatic Synaptic Scaling of AMPA Receptors. *Neuron* *52*, 475–484.
- 691 Sherman, S.M., and Spear, P.D. (1982). Organization of visual pathways in normal and visually deprived
692 cats. *Physiol Rev* *62*, 738–855.
- 693 Steward, O., Matsudaira Yee, K., Farris, S., Pirbhoy, P.S., Worley, P., Okamura, K., Okuno, H., and Bito, H.
694 (2017). Delayed Degradation and Impaired Dendritic Delivery of Intron-Lacking EGFP-Arc/Arg3.1 mRNA
695 in EGFP-Arc Transgenic Mice. *Frontiers in Molecular Neuroscience* *10*, 435.
- 696 Tagawa, Y., Kanold, P.O., Majdan, M., and Shatz, C.J. (2005). Multiple periods of functional ocular
697 dominance plasticity in mouse visual cortex. *Nature Neuroscience* *8*, 380–388.
- 698 Torrado Pacheco, A., Tilden, E.I., Grutzner, S.M., Lane, B.J., Wu, Y., Hengen, K.B., Gjorgjieva, J., and
699 Turrigiano, G.G. (2019). Rapid and active stabilization of visual cortical firing rates across light-dark
700 transitions. *Proc Natl Acad Sci U S A* *116*, 18068–18077.
- 701 Tzingounis, A. V., and Nicoll, R.A. (2006). Arc/Arg3.1: Linking Gene Expression to Synaptic Plasticity and
702 Memory. *Neuron* *52*, 403–407.
- 703 Vazdarjanova, A., Ramirez-Amaya, V., Insel, N., Plummer, T.K., Rosi, S., Chowdhury, S., Mikhael, D.,
704 Worley, P.F., Guzowski, J.F., and Barnes, C.A. (2006). Spatial exploration induces ARC, a plasticity-related
705 immediate-early gene, only in calcium/calmodulin-dependent protein kinase II-positive principal
706 excitatory and inhibitory neurons of the rat forebrain. *The Journal of Comparative Neurology* *498*, 317–
707 329.

- 708 Veyrac, A., Besnard, A., Caboche, J., Davis, S., and Laroche, S. (2014). The Transcription Factor
709 Zif268/Egr1, Brain Plasticity, and Memory. *Progress in Molecular Biology and Translational Science* *122*,
710 89–129.
- 711 Wang, G., Xie, H., Hu, Y., Chen, Q., Liu, C., Liu, K., Yan, Y., and Guan, J.-S. (2021). Egr1-EGFP transgenic
712 mouse allows in vivo recording of Egr1 expression and neural activity. *J Neurosci Methods* *363*, 109350.
- 713 Wang, K.H., Majewska, A., Schummers, J., Farley, B., Hu, C., Sur, M., and Tonegawa, S. (2006). In vivo
714 two-photon imaging reveals a role of arc in enhancing orientation specificity in visual cortex. *Cell* *126*,
715 389–402.
- 716 Waung, M.W., Pfeiffer, B.E., Nosyreva, E.D., Ronesi, J.A., and Huber, K.M. (2008). Rapid Translation of
717 Arc/Arg3.1 Selectively Mediates mGluR-Dependent LTD through Persistent Increases in AMPAR
718 Endocytosis Rate. *Neuron* *59*, 84–97.
- 719 Weng, F.-J., Garcia, R.I., Lutz, S., Alviña, K., Zhang, Y., Dushko, M., Ku, T., Zemoura, K., Rich, D., Garcia-
720 Dominguez, D., et al. (2018). Npas4 Is a Critical Regulator of Learning-Induced Plasticity at Mossy Fiber-
721 CA3 Synapses during Contextual Memory Formation. *Neuron*.
- 722 Widmer, F.C., O'Toole, S.M., and Keller, G.B. (2022). NMDA receptors in visual cortex are necessary for
723 normal visuomotor integration and skill learning. *ELife* *11*, e71476.
- 724 Xie, H., Liu, Y., Zhu, Y., Ding, X., Yang, Y., and Guan, J.-S. (2014). In vivo imaging of immediate early gene
725 expression reveals layer-specific memory traces in the mammalian brain. *Proceedings of the National*
726 *Academy of Sciences* *111*, 2788–2793.
- 727 Yamada, Y., Hada, Y., Imamura, K., Mataga, N., Watanabe, Y., and Yamamoto, M. (1999). Differential
728 expression of immediate-early genes, c-fos and zif268, in the visual cortex of young rats: effects of a
729 noradrenergic neurotoxin on their expression. *Neuroscience* *92*, 473–484.
- 730 Yap, E.-L., and Greenberg, M.E. (2018). Activity-Regulated Transcription: Bridging the Gap between
731 Neural Activity and Behavior. *Neuron* *100*, 330–348.
- 732 Yasoshima, Y., Sako, N., Senba, E., and Yamamoto, T. (2006). Acute suppression, but not chronic genetic
733 deficiency, of c-fos gene expression impairs long-term memory in aversive taste learning. *Proceedings of*
734 *the National Academy of Sciences of the United States of America* *103*, 7106–7111.
- 735 Yassin, L., Benedetti, B.L., Jouhannau, J.S., Wen, J.A., Poulet, J.F.A., and Barth, A.L. (2010). An
736 Embedded Subnetwork of Highly Active Neurons in the Neocortex. *Neuron* *68*, 1043–1050.
- 737 Zmarz, P., and Keller, G.B. (2016). Mismatch Receptive Fields in Mouse Visual Cortex. *Neuron* *92*, 766–
738 772.
- 739